

Thermal conductivity of U_2Ru_2Sn single crystal

This article has been downloaded from IOPscience. Please scroll down to see the full text article.

2008 J. Phys.: Condens. Matter 20 085205

(<http://iopscience.iop.org/0953-8984/20/8/085205>)

View [the table of contents for this issue](#), or go to the [journal homepage](#) for more

Download details:

IP Address: 129.252.86.83

The article was downloaded on 29/05/2010 at 10:36

Please note that [terms and conditions apply](#).

Thermal conductivity of $\text{U}_2\text{Ru}_2\text{Sn}$ single crystal

J Mucha¹, H Misiorek¹, R Troć¹ and B Coqblin²

¹ W Trzebiatowski Institute for Low Temperature and Structure Research, Polish Academy of Science, PO Box 1410, 50-950 Wrocław 2, Poland

² Laboratoire de Physique des Solides, UMR 8502, CNRS, Université Paris-Sud, 91405 Orsay, France

E-mail: j.mucha@int.pan.wroc.pl

Received 19 November 2007, in final form 2 January 2008

Published 1 February 2008

Online at stacks.iop.org/JPhysCM/20/085205

Abstract

The thermal conductivity and the Lorenz function have been studied, along the two crystallographic directions a and c in the temperature range of 5–300 K, in a single crystal of the compound $\text{U}_2\text{Ru}_2\text{Sn}$, which behaves as a weak Kondo semiconductor with a gap of order 150 K. The observed large anisotropy results from both the considerable difference in the lattice parameters of the tetragonal structure and the difference in the type of thermal conductivity, i.e. crystal and quasi-amorphous ones. The contribution of bipolarons in the thermal conductivity confirms the semiconducting character of this compound. The presented results of the thermal conductivity of a uranium compound, which does not exhibit magnetic order, complete the examinations of the influence of phase transitions on heat transport in the antiferromagnetic $\text{UNi}_{0.5}\text{Sb}_2$ (Mucha *et al* 2006 *J. Phys.: Condens. Matter.* **18** 3097) and ferromagnetic UCu_2Si_2 compounds (Mucha *et al* 2008 *Solid State Commun.* at press).

1. Introduction

$\text{U}_2\text{Ru}_2\text{Sn}$, having the tetragonal U_3Si_2 -type structure, belongs to a group of a few recently recognized materials that are classified as Kondo insulators or alternatively heavy-fermion semiconductors [1]. All these compounds are mainly cerium ternary intermetallics and are non-magnetic down to the lowest temperatures.

The system considered here falls in the category where the magnetic moment is entirely suppressed by a large hybridization with the conduction electrons and reveals, therefore, the properties characteristic of an intermediate valence behaviour. Thus, this behaviour is in line with the temperature dependence of the magnetic susceptibility of $\text{U}_2\text{Ru}_2\text{Sn}$ measured for both crystallographic directions a and c of the tetragonal symmetry. It was found to be distinctly anisotropic and goes through a broad maximum at temperatures 170 K and 190 K, respectively [2, 3]. As shown in [3], it was possible to fit the experimental data with the inter-configuration fluctuation (ICF) model [4], in which a valence fluctuation system is characterized by two energy parameters, namely an energy difference E_{cx} related to the energies of the U^{4+} and U^{3+} free ions, and the so-called valence fluctuation temperature T_{sf} . One important

result characterizing the mixed valence behaviour is that the susceptibility measured along both directions a and c follows a Curie–Weiss law at temperatures above ~ 300 K with the effective magnetic moment being close to the free ion values of both U^{4+} ($5f^2$) and U^{3+} ($5f^3$).

The resistivity of $\text{U}_2\text{Ru}_2\text{Sn}$ [2] is also highly anisotropic and yields a band-gap E_{g} according to an activation-like description that differs by two orders of magnitude depending on the current direction. Several measurements made on the polycrystalline sample [5] support the interpretation of the physics of $\text{U}_2\text{Ru}_2\text{Sn}$ in terms of the formation of an energy gap, $E_{\text{g}} = 140\text{--}160$ K. In this compound the magnetic, thermodynamic, NMR and transport properties indicate various magnitudes of the energy gap E_{g} . Different values of the energy gap have been obtained by different experiments: values of order 510–570 K are expected from the value of $3 \cdot \chi_{T \text{ max}}$ [3] derived by the magnetic susceptibility and are considerably larger than those determined from the electrical resistivity [2, 5, 6]. The large values are supported by a spin excitation gap of ~ 60 meV (660 K), which has been reported [7] from the inelastic neutron measurements.

On the other hand, the recently reported far-infrared optical investigation of $\text{U}_2\text{Ru}_2\text{Sn}$ [8] shows a pronounced suppression of E_{g} at energies below 60 meV and temperatures

below 200 K. The observed decrease in the reflectivity $R(\omega)$ shows peculiarities typical of Kondo insulators. The deduced value of Δ_{opt} corresponds here to roughly 700 K, without any shift in energy when reducing temperature. However, usually, as pointed out above, the gap is only visible at temperatures below 150 K. Hence, the temperature dependence of the far-infrared reflectivity in $\text{U}_2\text{Ru}_2\text{Sn}$ is interpreted in terms of a pseudo-gap formation due to the temperature dependent 5f-conduction electron hybridization [8]. Electronic structure and photoemission studies of $\text{U}_2\text{Ru}_2\text{Sn}$ [9], as well as NMR studies [10, 11], have shown that the density of states (DOS) in the vicinity of the Fermi energy, E_F , has a V-shaped pseudo-gap and the satellite structure of the 4f core lines supports the view of the dual nature of the 5f electrons in this compound, i.e. showing both localized and itinerant behaviour. Recent NMR measurements carried out on single crystals (or oriented micro-crystallites) of Knight shift $K(T)$ for $H \parallel c$ have indicated a change of slope at 150 K with a greater decrease below [11]. Thus, we can conclude that the value of the gap observed in $\text{U}_2\text{Ru}_2\text{Sn}$ is typically of order 150 K and that the origin of the gap is probably due to the 5f-conduction electron hybridization in this compound, although its heavy-fermion character is small [5].

In this paper, the thermal conductivity results made on a single-crystalline sample of $\text{U}_2\text{Ru}_2\text{Sn}$ are presented. The results of thermal conductivity and electrical resistivity [2] were fitted to the equations derived from the Wiedemann–Franz law in order to separate the electronic κ_e and phonon κ_{ph} components from the total thermal conductivity κ .

2. Experimental details

A $\text{U}_2\text{Ru}_2\text{Sn}$ single crystal was prepared using the Czochralski method. The starting materials were U (99.89), Ru (99.99) and Sn (99.999), with the purity expressed in weight per cent in parentheses. No annealing was performed on the prepared ingot. Following orientation by Laue x-ray back-reflection, the pieces were cut by tungsten wire into specimens of appropriate geometry and tetragonal orientation.

The thermal conductivity was measured using the stationary heat flux method in the temperature range 5–300 K. The experimental set-up and the measurement procedure have been described in detail in [12]. The temperature difference (ΔT) along the sample was in the range 0.1–0.5 K. Particular care was taken to avoid a parasitic heat transfer between the sample and its environment. The measurement error was below 2% and the surplus error, estimated from the scatter in the measurement points, did not exceed 0.3%. The electrical resistivity results were taken from [2], where they were obtained on single crystals by using the four-probe dc method between 4 and 300 K.

3. Results and discussion

The total thermal conductivity of non-magnetic materials like $\text{U}_2\text{Ru}_2\text{Sn}$ is generally assumed to be composed of several contributions like electronic, phonon, bipolaron and excitonic ones, depending on the kind of heat carriers. So the total

thermal conductivity κ can be expressed by $\kappa = \kappa_e + \kappa_{\text{ph}} + \kappa_{\text{bip}} + \kappa_{\text{exc}}$ [13, 14]. For metals, the electronic conductivity κ_e is dominant, but it is more difficult to deduce the electronic conductivity in the present case of semiconductors. Previous results on the polycrystalline $\text{U}_2\text{Ru}_2\text{Sn}$ compound [5] have given electrical resistivity and the thermal conductivity which are very different for the two considered samples and then the Lorenz number has also been deduced. It appears there that the Lorenz number is first of all for the two samples and has a huge value, especially at low temperature below approximately 160 K. The authors of [5] have concluded that the thermal conductivity is dominated by phonons and that the enhancement of the Lorenz number is related to the opening of the gap at the Fermi level. Moreover, their deduced net resistivity, taken, as usual, equal to the difference between the total resistivities of $\text{U}_2\text{Ru}_2\text{Sn}$ and its non-magnetic equivalent $\text{Th}_2\text{Ru}_2\text{Sn}$ turns out to be very close to the total resistivity of $\text{U}_2\text{Ru}_2\text{Sn}$.

Thus, it is not easy to deduce here the electronic contribution to the thermal conductivity, but, in order to study the different contributions, we make here the crude approximation of taking the temperature variation of $\kappa_e(T)$ directly from the Wiedemann–Franz (WF) law, i.e. $\kappa_e(T) = (L_0 \times T)/\rho(T)$, where we take for $\rho(T)$ the total resistivity for the two *a*- and *c*-directions. L_0 is here the Lorenz number, given by $L_0 = \pi^2/3(k_B/e)^2 = 2.45 \times 10^{-8} \text{ W } \Omega \text{ K}^{-2}$, k_B the Boltzmann constant and e the electron charge. Then, the phonon conductivity, κ_{ph} , is described by the Debye equation

$$\kappa_{\text{ph}} = GT^3 \int_0^{\Theta/T} \frac{x^4}{\tau^{-1} \sinh^2(x/2)} dx, \quad (1)$$

where $x = \hbar\omega/k_B T$, G is a constant and τ^{-1} is the sum of the inverse relaxation times of different kinds of phonon scattering: $\tau^{-1} = \Sigma \tau_i^{-1}$, where $\tau_i = \tau_b, \tau_d$ and τ_U are relaxation times for phonon scattering on the sample border defects and impurities and finally in the Umklapp ('U') processes. We write $\tau_b^{-1} = B$ and the other relaxation times of scattering mechanisms are mainly dependent on frequency ω and temperature, i.e. $\tau_d^{-1} = D\omega^4$ and $\tau_U^{-1} = U\omega^2 T \exp(-\theta_D/3T)$, where B, D, U are constants [15].

At very low temperatures, where the mean free path of phonons is comparable with the size of a crystal, the dominant role is played by the scattering of phonons on the crystal borders, which leads to $\kappa_{\text{ph}} \propto T^3$. In the intermediate temperature region, the dominant scattering is of 'U' type. The latter is reflected by exponential temperature dependence of the lattice thermal conductivity. At high temperatures, $T \geq \theta_D$, this exponential dependence changes into the Leibfried–Schlömann expression, i.e. where $\kappa_{\text{ph}} \propto T^{-1}$, which is valid for pure dielectrics only. For the other contributions, such as the bipolar (κ_{bip}) and excitonic (κ_{exc}) ones, the heat transport is well described in reviews [16] and [13].

Figure 1 presents the temperature dependence of the thermal conductivity for both the main crystallographic directions *c* and *a*, but the thermal conductivity along the *c* axis always remains larger than that along the *a* axis. The inset of figure 1 gives the temperature dependence of the ratio

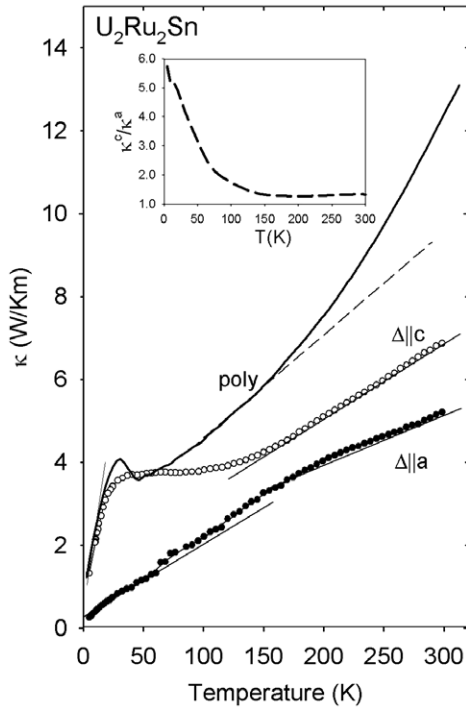


Figure 1. The temperature dependence of the thermal conductivity along the *a* and *c* directions as well as for the polycrystalline sample of U_2Ru_2Sn , the data of which were taken from [5]. The inset displays the temperature dependence of the ratio κ^c/κ^a .

κ^c/κ^a , which remains small, of order 1.2, in the temperature range 160–300 K, but increases with decreasing temperature and reaches a large value of order 6 at very low temperatures. However, a distinct change between $\kappa^c(T)$ and $\kappa^a(T)$ is observed between 25 and 160 K. As clearly shown in figure 1, $\kappa^c(T)$ initially rises sharply and then goes through a plateau around 30 K. On the other hand, $\kappa^a(T)$ rises almost linearly when temperature is increased. Both curves show an inflection point T_{infl} at about 150 K, and above roughly 200 K $\kappa^c(T)$ and $\kappa^a(T)$ are increasing linearly with almost the same slope.

We also present in figure 1 the thermal conductivity $\kappa_{\text{poly}}(T)$ of a polycrystalline sample in the temperature range 5–300 K; this result is taken from the work of Tran *et al* [5] and we have chosen here the results of the sample which has the highest value of $\kappa_{\text{poly}}(T)$. At low temperatures up to 10 K, both the values and the temperature variation of this sample are close to our results on $\kappa^c(T)$. Above this temperature, a difference is observed with a cusp around 25 K and a wide minimum around $T_{\text{min}} = 45$ K. At higher temperatures, $\kappa_{\text{poly}}(T)$ varies linearly, similarly to $\kappa^a(T)$ between 60 and 160 K, with a similar slope, but above 200 K it deviates from such a run due probably to the heat radiation effect [17]. The cusp and the wide minimum observed in the curve of $\kappa_{\text{poly}}(T)$ are not understood at present.

Figure 2, using the double logarithmic scales, gives the separation of the total thermal conductivity κ into the electronic κ_e and phonon κ_{ph} parts for both the main crystallographic directions by using the Wiedemann–Franz (WF) law as explained before.

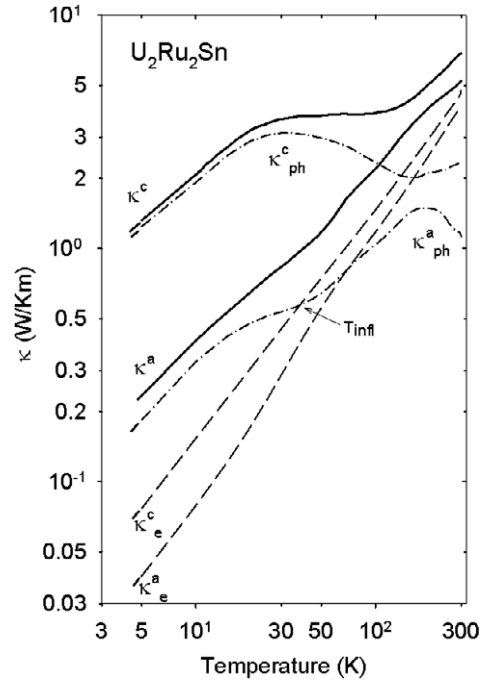


Figure 2. The temperature dependence (in double logarithmic scales) of the electronic and phonon parts of the thermal conductivity, as explained in text.

Let us discuss successively the electronic and phonon parts of the total thermal conductivity of the U_2Ru_2Sn compound. First, the electronic parts $\kappa_e^{a,c}(T)$ for both axes *a* and *c* behave almost linearly in the whole range of temperatures. In addition, for the *a* axis, an inflection point is detected at about $T_{\text{infl}} = 30$ K. This means that these electronic contributions to $\kappa(T)$ are temperature dependent with slightly different *T* powers *n* for the *c*-direction and *n*₁ or *n*₂ for the *a*-direction. This also indicates that the electrons involved in this type of heat transport are scattered mainly by impurities and defects on the lattice [14]. However, the values of $\kappa_e(T)$ at very low temperatures are very small and correspond to about 1–3% of the total heat transport. At higher temperatures ($T > 100$ K), these contributions are significantly changed and reach 50% of the total thermal conductivity κ .

The theoretical interpretation of the thermal conductivity of anomalous rare-earth and actinide compounds is more difficult to perform than that of the electrical resistivity. A clear interpretation has been given for the electronic contribution to the thermal conductivity of Kondo compounds with cerium, ytterbium or other anomalous rare earths [18, 19]. However, the U_2Ru_2Sn compound is not magnetic and is characterized by an intermediate valence behaviour [3]. The temperature dependence of the thermal conductivity of nearly magnetic metals and in particular of plutonium metal had been performed by using the spin fluctuation model [20]. The electronic thermal resistivity, which has been computed in this paramagnon model, increases linearly with temperature, then passes through a maximum corresponding roughly to the spin fluctuation temperature and finally decreases at higher temperatures. The resulting electronic thermal conductivity, computed in this model, presents an almost linear increase at

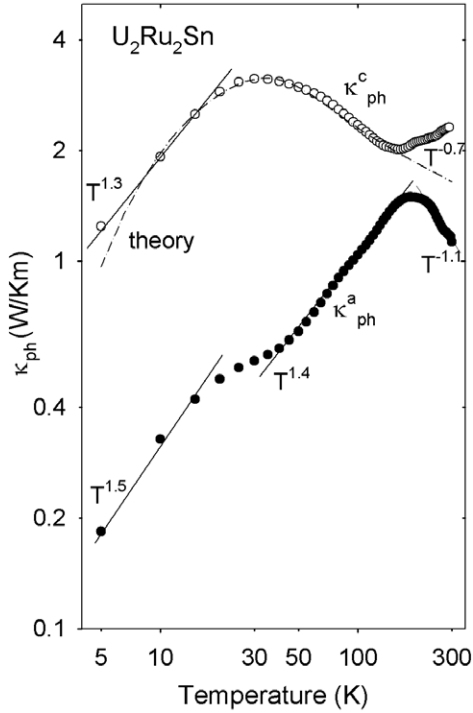


Figure 3. The phonon thermal conductivity, κ_{ph} , along the two a and c axes as a function of temperature, in a double logarithmic scale. The dashed curve is a fit to equation (1). Note that $\kappa(T)$ at higher temperatures varies according to the L–S dependence, i.e. $\kappa(T)$ is proportional to T^{-1} .

high temperatures above a minimum corresponding roughly to the spin fluctuation temperature; this paramagnon model had accounted for the very large thermal resistivity observed in plutonium metal [20]. Our present results on the $\text{U}_2\text{Ru}_2\text{Sn}$ compound show an almost linear increase of the electronic thermal conductivity but without any minimum even at very low temperatures; the values of the electronic parts $\kappa_e^{a,c}(T)$ are typically of the same order of magnitude as the experimental values quoted for plutonium metal. Thus, we can conclude that the electronic thermal conductivity of the $\text{U}_2\text{Ru}_2\text{Sn}$ compound can be at least qualitatively understood within the spin fluctuation model, which is well appropriate for describing this type of compounds.

Let us discuss now the phonon contribution to the thermal conductivity. A quite different contribution to $\kappa(T)$ is observed along the different crystallographic axes for the temperature dependence of $\kappa_{\text{ph}}(T)$. Surprisingly, the $\kappa_{\text{ph}}(T)$ variation along the c direction in the temperature range 5–160 K is typical of pure dielectrics [21], i.e. $\kappa_{\text{ph}}^c(T)$ increases with increasing temperature as $T^{1.3}$ from 5 to 20 K and then passes through a wide maximum at about $T_{\text{max}} \approx 30$ K. Above this temperature, this phonon part decreases as $T^{-0.7}$ down to 160 K according to the Leibfried–Schlomann (L–S) expression (figure 3). Above this temperature, κ_{ph}^c rises with temperature in a way similar to that of semimetals and semiconductors, in which there is an important bipolaron contribution.

On the other hand, $\kappa_{\text{ph}}^a(T)$ varies otherwise than $\kappa_{\text{ph}}^c(T)$, increasing firstly as $T^{1.5}$, then going through an inflection point

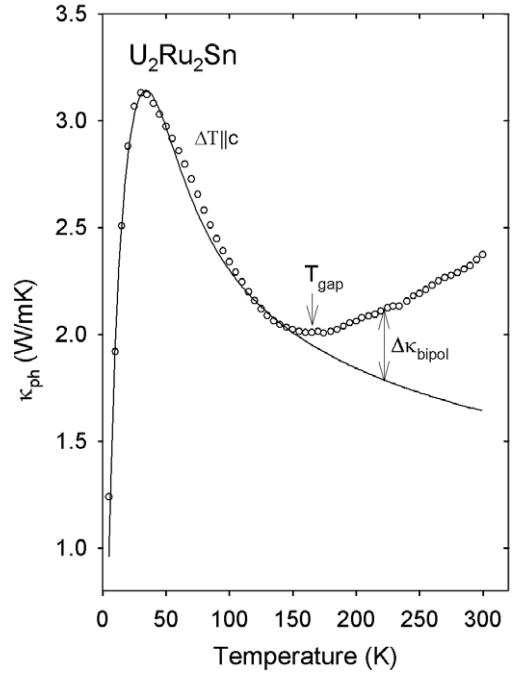


Figure 4. Plot versus temperature of the phonon contribution κ_{ph}^c of the thermal conductivity along the c direction and of the solid line corresponding to an extrapolated $T^{-0.7}$ decrease above 150 K. The observed difference between these two curves has been attributed to the bipolar contribution to the phonon thermal conductivity.

$T_{\text{infl}} = 30$ K, which cannot be fitted by the L–S expression, in spite of the similar power law observed along the a and c axes in the initial increase at very low temperatures. Then, $\kappa_{\text{ph}}^a(T)$ increases as $T^{1.4}$ with increasing temperature up to $T = 160$ K (see figure 3). It is interesting to note that the temperature dependence of κ_{ph}^a in the range 5–160 K is like that of amorphous materials [22] and could be considered as that observed in a ‘quasi-amorphous’ material. At the same time, we are unable to explain this behaviour and why at temperatures above 160 K the resulting thermal conductivity behaves typically as for pure dielectrics.

As follows from the different types of determination of E_g [5], the temperature of 160 K, found in this paper, is close to the energy gap obtained in the electronic structure at E_F existing in this compound. In our case, the possible scenario is as follows: at $T \approx 160$ K, the mean free path of the phonons, generated by the ‘amorphous-like phase’, is small and independent of temperature, while this path of free phonons in the ‘crystal phase’ is considerably larger but is vanishing slowly with increasing temperature, leading finally to the $1/T$ dependence of $\kappa_{\text{ph}}^a(T)$ above 160 K.

Figure 3 presents in double logarithmic scale the temperature dependence of the phonon thermal conductivity, $\kappa_{\text{ph}}(T)$, for the two main crystallographic directions. The dashed line gives a fit of the experimental data by the Debye equation (1). It is clearly seen that equation (1) in the temperature range 10–160 K describes reasonably well the phonon contribution to κ . The fit yields the following parameters: the constants B , D and U , the Debye temperature θ_D and the sound velocity v_{ph} . However, the value of θ_D found

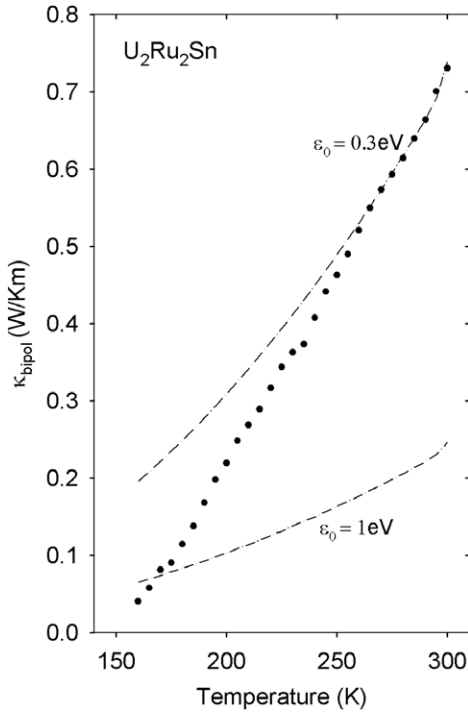


Figure 5. The black points are the experimental data of the bipolar thermal conductivity deduced from figure 4. The calculated values of the bipolar contribution are plotted by taking the different energies $\varepsilon_0 = 0.3$ or 1 eV, with a temperature gradient ΔT parallel to the c axis.

from this fitting takes a much larger value than that found from the heat capacity, i.e. $\theta_D = 210$ K [5].

As already established, the Debye expression does not take into account the real processes responsible for the contribution to the heat resistance, e.g. many-phonon, real dispersion of the acoustic and optical phonons, separation between the transverse and longitudinal modes and their influence on the heat transport. In the classical models, the quantities existing in an expression of the phonon heat transport vary with the temperature, giving a resulting dependence of $\kappa_{ph}(T)$. At low temperatures ($T \ll \theta_D$), phonons are scattered mainly by crystal boundaries and $\kappa_{ph} \sim T^3$. At $T > \theta_D$, the phonon–phonon scattering leads to a temperature dependence of $\kappa_{ph} \sim T^{-1}$. At intermediate temperatures, but with $T > T_{max}$, the dominant processes are of scattering phonon–phonon ‘Umklapp’ (U processes) type, yielding the dependence, $\kappa_{ph} \sim \exp(\theta_D/aT)$ [14].

However, in the case of existing dislocations in a crystal and of other phonon–phonon scattering mechanisms in the heat transport, there are deviations from the expression (1). These are well seen in figures 3 and 4. Especially at temperatures $T > 160$ K, one can see a clear deviation from the power dependence $\kappa_{ph} \sim T^{-0.7}$ and a strong rise of the thermal conductivity κ_{ph}^c with increasing temperature (figure 4), due to bipolar heat transport. The description of the bipolar separation in the heat transport is given in works [13, 16, 23]. A bipolaron is the electron–hole system having the binding energy ε_0 . We assume that electrons and holes are scattered independently and their relaxation time is $\tau \sim \varepsilon^r$ ($r = -0.5$ in the

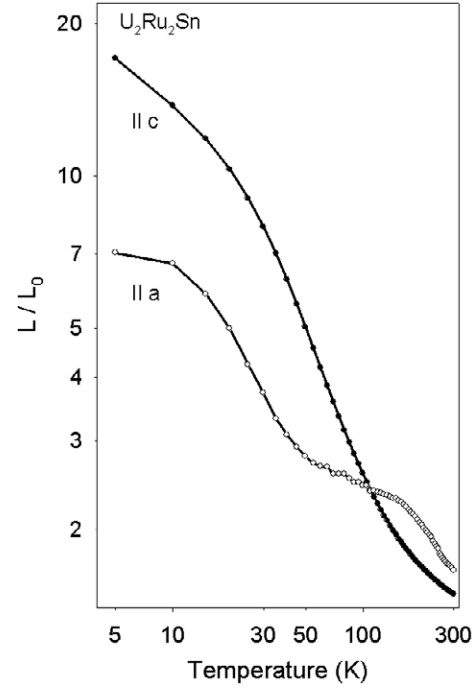


Figure 6. The temperature dependence of the Lorenz ratio L/L_0 for both crystallographic directions a and c in double logarithmic scales. $L_0 = 2.45 \times 10^{-8} \text{ W } \Omega \text{ K}^{-2}$.

case of acoustic phonons). Taking into account this procedure, we were able to separate the bipolar contribution to the thermal conductivity of U_2Ru_2Sn from the $\kappa_{ph}^c(T)$ dependence (figure 4).

In figure 5, the dashed lines are drawn for two values of ε_0 . The black points are the results of the obtained bipolar thermal conductivity in the range 160–300 K, taken as the difference between the values of $\kappa_{ph}^c(T)$ and the calculated one as explained before and shown in figure 4. This difference describing the bipolar part of the thermal conductivity is shown in figure 5, where we have also plotted the calculated curves for ε_0 equal to 0.3 and 1 eV. For comparison, the corresponding values are $3 \times 10^{-3} \text{ eV} < \varepsilon_0 < 1 \times 10^{-3} \text{ eV}$ for $UNi_{0.5}Sb_2$ [16] and $\varepsilon_0 = 2.3 \times 10^{-2} \text{ eV}$ for $ErPdSb$ [24]. It is clear that the determination of κ_{bipol} was only possible by using some rough simplifications, for example the equality of the effective masses of electrons and holes, $m_n^* = m_p^*$ (while usually one has $m_p^* \gg m_n^*$) and also of the mobilities $\mu_p^* = \mu_n^*$ (while usually one has $\mu_n^* \gg \mu_p^*$), and finally a simple parabolic shape of the overlapping electron and hole bands [23]. Besides, U_2Ru_2Sn is a Kondo semiconductor [6] and one should take into account the additional heat resistance connected with the conduction electrons scattered by localized 5f electrons of uranium ions.

The temperature dependence of the reduced Lorenz function along both crystallographic directions is shown in figure 6, which shows very large values of the Lorenz function. The enhancement of the Lorenz function at low temperatures is probably connected with the occurrence of the gap of order 150 K and with the low-angle scattering electron–phonon ($q_{ph} \ll k_F$) influence on the electron conduction heat transport [21]. This comes from the fact that the probability of

such a scattering rises with lowering temperature, because the excitations of long-wave phonons are more important at low temperatures.

4. Conclusions

The thermal conductivity and the Lorenz function are studied here for the first time using a single crystal of U_2Ru_2Sn oriented along both tetragonal crystallographic directions a and c , in the wide temperature range 5–300 K. We have observed a large anisotropy in the thermal conductivity, as well as different characters of the low temperature dependences, i.e. ‘crystalline’ along the c axis and ‘quasi-amorphous’ along the a axis. We have then separated the electron and phonon parts by using the WF law, then determined the Lorenz function and finally extracted the bipolar contribution at temperatures above $T = 160$ K, which corresponds to the energy of the (pseudo-) gap E_g . The analysis of the obtained results may point out the Kondo semiconductor character of this compound. We think that the measurements of the transport properties under magnetic field will be important to study the heat transport phenomena taking place in U_2Ru_2Sn .

Acknowledgments

RT is grateful to Professor I A Smirnov for stimulating discussions and to Professor T Komatsubara for his help in obtaining single crystals of U_2Ru_2Sn . BC thanks Professor P Riseborough for interesting discussions and the European COST Action P16 (Emergent Behaviour in Correlated Matter) for its strong support.

References

- [1] Riseborough P S 2000 *Adv. Phys.* **49** 257
 [2] Strydom A M and Troć R 2003 *Solid State Commun.* **126** 207

- [3] Troć R 2006 *Physica B* **378–380** 985
 [4] Sales B C and Wohlleben D K 1975 *Phys. Rev. Lett.* **35** 1240
 [5] Tran V H, Paschen S, Rabis A, Senthilkumaran N, Baenitz M and Steglich F 2003 *Phys. Rev. B* **67** 075111
 [6] Plessis P de V Du, Strydom A M, Troć R and Menon L 2001 *J. Phys.: Condens. Matter* **13** 8375
 [7] McEwen K A, Adroja D T, Hillier A D, Park J G and Bewley R I 2004 *SCES04 (Karlsruhe, July)*
 [8] Sichelschmidt I, Voevodin V, Mydosh I A and Steglich F 2007 *J. Magn. Magn. Mater.* **310** 434
 [9] Chełkowska G, Markowski I A, Szajek A, Stępień-Damm J and Troć R 2003 *Eur. Phys. J. B* **35** 349
 [10] Baenitz M, Rabis A, Paschen S, Senthilkumaran N, Steglich F, Tran V H, Plessis P de V Du and Strydom A M 2003 *Physica B* **329–333** 545
 [11] Rajaran A K, Rabis A, Baenitz M, Gippins A A, Morozowa E N, Mydosh I A and Steglich F 2005 *Physica B* **359–361** 997
 [12] Jeżowski A, Mucha J and Pompe G 1987 *J. Phys. D: Appl. Phys.* **20** 1500
 [13] Smirnov I A and Oskotski V S 1993 *Handbook on the Physics and Chemistry of Rare Earths* vol 16, ed K A Gschneider and L Eyring (Amsterdam: North-Holland) p 116
 [14] Berman R 1976 *Thermal Conductivity in Solids* (Oxford: Clarendon)
 [15] Callaway J 1959 *Phys. Rev.* **113** 1046
 [16] Mucha J, Misiorek H, Troć R and Bukowski Z 2006 *J. Phys.: Condens. Matter* **18** 3097
 [17] Mucha J, Dorbolo S, Bougrine H, Durczewski K and Ausloos M 2000 *Cryogenics* **44** 145
 [18] Bhattacharjee A K and Coqblin B 1988 *Phys. Rev. B* **38** 338
 [19] Kletowski Z and Coqblin B 2005 *Solid State Commun.* **135** 711
 [20] Jullien R and Coqblin B 1975 *J. Low Temp. Phys.* **19** 59
 [21] Ziman J M 1960 *Electrons and Phonons* (Oxford: Clarendon)
 [22] Phillips W A (ed) 1981 *Amorphous Solids, Low-Temperature Properties* (Berlin: Springer)
 [23] Golubkov A V, Parfenèva L S, Smirnov I A, Misiorek H, Mucha J and Jeżowski A 2000 *Phys. Solid State* **42** 1357
 [24] Gofryk K, Kaczorowski D, Plackowski T, Mucha J, Leithe-Jasper A, Schnelle W and Grin Yu 2007 *Phys. Rev. B* **75** 224426
 [25] Mucha J, Misiorek H, Troć R, Pękała M, Fagnard J-F, Vanderbemden Ph and Ausloos M 2008 *Solid State Commun.* at press